§3. Summary of Density Comparison

This is a preliminary analysis of the dimuon and single muon event rates for the density comparison where the emphasis has been placed on equal geometrical acceptance. The momentum analysis of the data is incomplete at this time.

The nonprompt background is a steep function of the penetration requirement. For the high density target the nonprompt background accounts for 34% of the signal with the penetration requirement of 1.9 m of steel and is consistent with no background when a penetration of 3.8 m of steel is required. The prompt rates obtained from the extrapolation to infinite target decrease with increasing penetration as expected.

References

1. B. C. Barish *et al.*: Phys. Rev. Letters **39** (1977) 981.
2. M. Holder *et al.*: Phys. Letters **69B** (1977) 377; **70B** (1977) 396.
3. A. Benvenuti *et al.*: Phys. Rev. Letters **38** (1977) 1183 and references listed there.
4. A. Benvenuti *et al.*: Phys. Rev. Letters **35** (1975) 1199.

PROC. 19th INT. CONF. HIGH ENERGY PHYSICS
TOKYO, 1978

B 5 Recent Results on Neutrino Reactions

A. K. MANN

Department of Physics, University of Pennsylvania, Philadelphia, PA 19104

I wish to report recent results from the new HPWF neutrino experiment (E-310) which now includes Rutgers and Ohio State University among the participating institutions. The plan of the talk is to discuss briefly new data on each of the reactions:

$$\bar{\nu}_\mu + N \to \mu^+ + X \quad (1)$$

$$\nu_\mu(\bar{\nu}_\mu) + N \to \mu^- + \mu^+ + X \quad (2)$$

$$\nu_\mu(\bar{\nu}_\mu) + N \to \mu^\mp + \mu^\mp + X \quad (3)$$

$$\nu_\mu + N \to \mu^- + \mu^- + \mu^+ + X \quad (4)$$

§1. $\bar{\nu}_\mu + N \to \mu^+ + X$

A year ago the world data on the energy dependence of y-distribution was as shown in Fig. 1, which contains all data available in August, 1977.

Here $B^\nu = -\int xF_3(x)\mathrm{d}x / F_2(x)\mathrm{d}x$ is the parameter conventionally used to describe the shape of y-distributions. In the quark parton model (QPM) with scale and charge symmetry invariance, which provide a good approximate representation of the data, $B^\nu = B^{\bar{\nu}}$ is related to the ratio of the charged current cross sections by

$$\sigma_c^{\bar{\nu}}/\sigma_c^{\nu} = (2 - B^{\bar{\nu}})/(2 + B^{\bar{\nu}}),$$

and to the fractional momentum carried by the antiquarks through

$$B^{\bar{\nu}} = 1 - 2\bar{Q}/(Q + \bar{Q}).$$

The conclusion drawn from Fig. 1 one year ago was that $B^{\bar{\nu}}$ was essentially independent of energy with a value of about 0.8 ever the region from a few to 200 GeV. This conclusion was based largely on the published data from the CDHS group as indicated in Fig. 1. It is now—one year later—clear that that conclusion was wrong because the CDHS data were wrong and because new data are available from other experiments.

The data at present—August, 1978—are shown in Fig. 2, which includes new results (based on 5200 $\bar{\nu}$ events) from HPWF (E-310), but omits a few earlier results with large error bars and the incorrect CDHS results. Figure 2 indicates a significant energy dependence of $B^{\bar{\nu}}$: below about 40 GeV, $B^{\bar{\nu}} = 0.82 \pm 0.05$, while above about 80 GeV, $B^{\bar{\nu}} = 0.63 \pm 0.06$; the detailed dependence of $B^{\bar{\nu}}$ on $E_{\bar{\nu}}$ is, however, not yet well delineated by the experimental data, and more precise results are need-

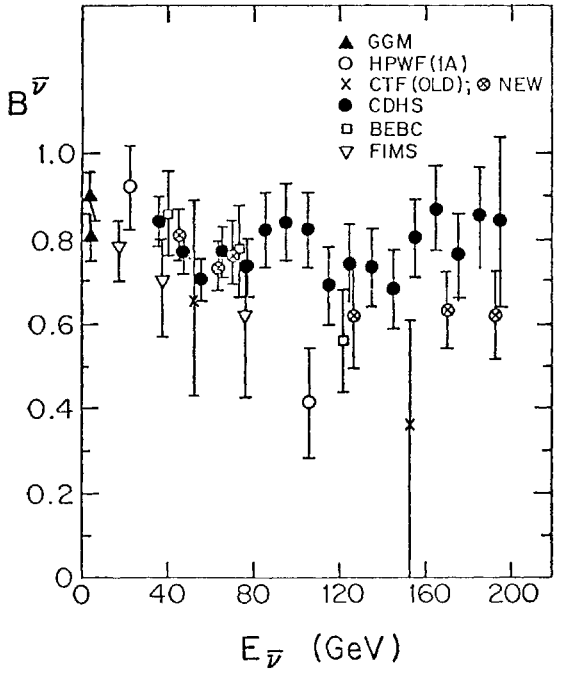

Fig. 1. Plot of $B^{\bar{\nu}}$ against $E_{\bar{\nu}}$ including all data published before August, 1977. $B^{\bar{\nu}}=-\int xF_3(x)dx/\int F_2(x)dx$ is the sole parameter that determines the shape of the inelasticity (y-) distributions.

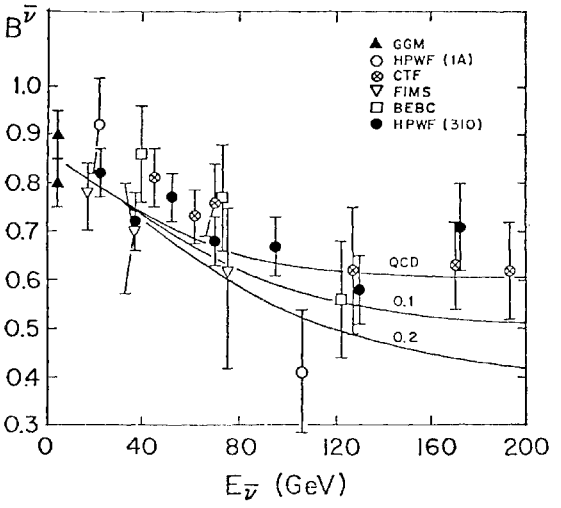

Fig. 2. Plot of $B^{\bar{\nu}}$ against $E_{\bar{\nu}}$ as of August, 1978. The "old" CTF data with large error bars and the CDHS data shown in Fig. 1 have been omitted here. The curves are from M. Barnett's talk at Neutrinos-78, and the numbers attached to them are values of $\sin^2\varphi$ in $(ub\sin\varphi)_R$.

ed in the energy region from 10 to 80 GeV. One likely interpretation of the energy dependence exhibited in Fig. 2 is given by asymptotic freedom corrections to the QPM in combination with charm particle production. The curve marked QCD in Fig. 2 is due to Barnett who has also estimated the effect on $B^{\bar{\nu}}$ of a b-quark of mass 5 GeV/c^2 coupled right-handedly to a u-quark with strength

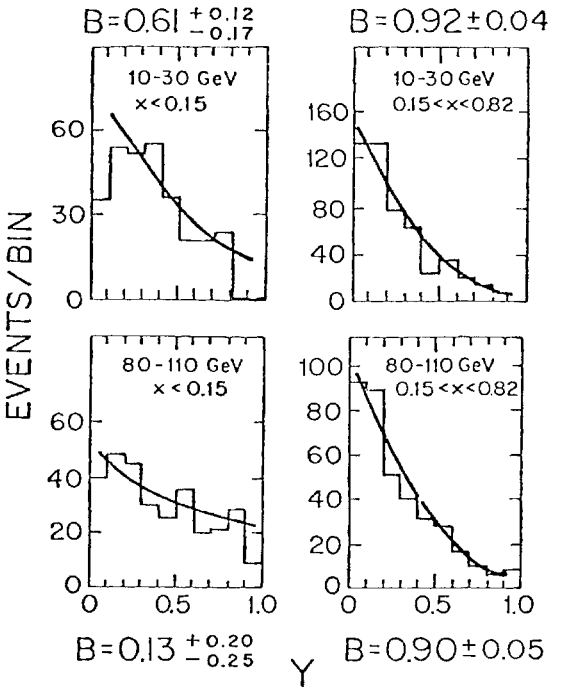

Fig. 3. Distributions in y at small and large x for two different regions in $E_{\bar{\nu}}$. The fits and values of $B^{\bar{\nu}}$ obtained are also shown.

given by $\sin\varphi$, as shown in the lower curves of Fig. 2. It appears from Fig. 2 that $\sin^2\varphi$ is probably less than 0.2, but this conclusion is subject to uncertainties in the QCD calculation as well as in the data. Nevertheless, it is important to attempt to determine the strength of any right-handed quark coupling, and this comparison of b-quark expectation with the $\bar{\nu}$ data needs to be refined in the future, at least until we know whether $\sin^2\varphi \ll \sin^2\theta_c$ or not.

There is shown in Fig. 3 y-distributions from E-310 for two energy intervals and two regions of the scaling variable x which indicates an appreciable difference of the y-distributions in the low-x (antiquark dominated) and high-x (valence quark dominated) regions. The detailed dependence of $(\bar{U}+\bar{S})/U$ on x (which is just $(1-B^{\bar{\nu}})/(1+B^{\bar{\nu}})$ *vs* x) is given in Fig. 4. Also shown in Fig. 4 is the best fit to the expression $\kappa(1-x)^{\gamma}/\sqrt{x}$, obtained by combining the phenomenological forms $\bar{U}(x)\sim(1-x)^{(n+\alpha)}$, $\bar{S}(x)\sim(1-x)^{(n+\beta)}$ and $U(x)\sim\sqrt{x}(1-x)^m$. The best fit yeilds $\gamma=5.8\pm1.0$, which is consistent with the values of α, β, n and m derived from analysis of e–N, μ–N and hadron-induced dilepton production experiments (see the talks of Fields and Lederman at this Conference).

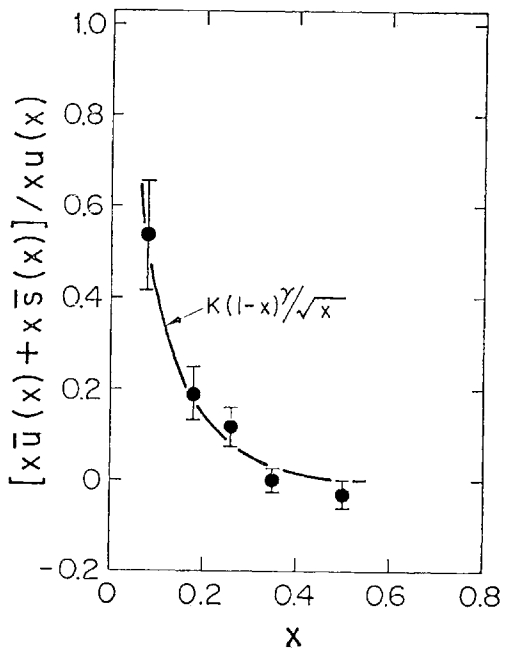

Fig. 4. Plot of the x-dependence of $(\bar{U}+\bar{S})/U$.

The conclusions concerning the reaction $\bar{\nu}_\mu+N\to\mu^++X$ may be summarized as follows.

1. *Energy dependence of* $B^{\bar{\nu}}$

$E_{\bar{\nu}}<40$ *GeV*

$B^{\bar{\nu}}=0.82\pm0.05\to\sigma_c^{\bar{\nu}}/\sigma_c^{\nu}=0.40\pm0.03$

$\bar{Q}/(Q+\bar{Q})=0.08\pm0.03$

consistent with e–p and μ–p scattering

$E_{\bar{\nu}}\gtrsim 80$ *GeV*

$B^{\bar{\nu}}=0.63\pm0.06\to\sigma_c^{\bar{\nu}}/\sigma_c^{\nu}=0.55\pm0.05$

$\bar{Q}/(Q+\bar{Q})=0.17\pm0.03$

2. *b-quark*

For $m_b\approx 5$ GeV/c^2 and $(ub\sin\varphi)_R$ present limit is

$$\sin^2\varphi\lesssim 0.02$$

3. *x-dependence of* $B^{\bar{\nu}}$

Increase of $\bar{Q}/Q$ in both x-regions with increasing $E_{\bar{\nu}}$

$x\lesssim 0.15$: sharp(?)

$x>0.15$: gradual

§2. $\nu_\mu(\bar{\nu}_\mu)+N\to\mu^-+\mu^++X$

Opposite sign dimuon production by neutrinos provided some of the earliest evidence for charm. Subsequent measurements have strengthened the interpretation that most opposite sign dimuon events arise from the production and semileptonic decay of charm particles, and the results presented here provide further quantitative confirmation of that interpretation.

The multimuon data reported here were acquired at Fermilab in three runs, using quadrupole triplet (QT) and sign-selected bare target beams (SSBT), with 400 GeV incident protons. The details of the data sample are shown in Table I.

The experimental distributions must be corrected for geometrical acceptance and counter efficiencies, and the background due to pion and kaon decay must be determined. The geometrical acceptance was obtained by rotating observed events in the azimuthal angle in the plane normal to the incident neutrino beam direction. Counter efficiencies were determined from single muon data. With a minimum momentum requirement of 5 GeV/c, there is a background of approximately 25% in the observed dimuon sample arising from pion and kaon decay. This was determined empirically using the different density targets to measure the dimuon rate as a function of hadronic absorption length. The result was consistent with a calculation, accurate to 25%, based on measured spectra and multiplicities of pions and kaons produced in neutrino interactions. The corrected experimental distributions and dimuon rates are compared with those predicted by a calculation based on the standard model of charm.

Table I. Multimuon data sample. The number of dimuon events for QT II is an estimate based on a small sample.

Beam	POT $\times 10^{18}$	Dimuons		Trimuons ($P_\mu>2$ GeV/c)	Tetramuon (candidates)
		opp. sign	same sign		
QT I	0.8	136	27	5	0
BTSS$_{\bar{\nu}}$	2.5	49	2	0	0
BTSS$_\nu$	0.4	63	19	3	1
QT II	3.7	~2000	~300	41	1

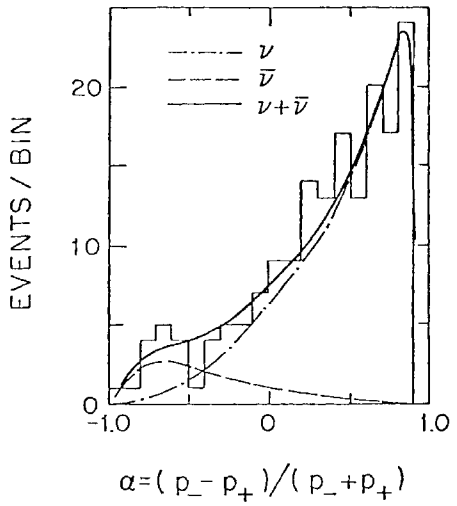

Fig. 5. Experimental distribution in the momentum asymmetry $\alpha \equiv (p_- - p_+)/(p_- + p_+)$ for the QT and SSBT (ν) dimuon samples. The curves are obtained from a charm model calculation.

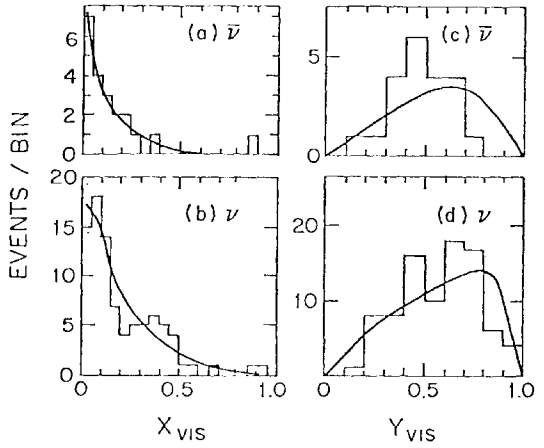

Fig. 6. Measured distributions in $x_{\rm vis}$ for (a) $\bar{\nu}$ and (b) ν, and in $y_{\rm vis}$ for (c) $\bar{\nu}$ and (d) ν (histograms) compared with the charm model calculation.

Figure 5 shows the distribution of the observed momentum asymmetry, $\alpha \equiv (p_- - p_+)/(p_- + p_+)$, for the data in the QT and SSBT(ν) samples of dimuon events with muon momenta above 5 GeV/c. The curves, obtained from a Monte Carlo calculation of charmed meson production and decay (and including π and K decay), show separately the contributions due to ν and $\bar{\nu}$ and their sum. The $\bar{\nu}$ contamination in the ν sample is reduced to 4% by requiring $\alpha > -0.3$ in the distributions presented below. Similarly the ν contamination in the SSBT($\bar{\nu}$) data is reduced to 8% by requiring $\alpha < 0.3$.

Figure 6 shows the distributions of $x_{\rm vis}$ and $y_{\rm vis}$ for ν and $\bar{\nu}$ events. In the standard charm model neutrinos can produce a charm quark from interactions with both strange (s) quarks in the sea and valence (d) quarks while antineutrinos produce charm essentially only from strange ($\bar{s}$) antiquarks. Note that the $\bar{\nu}$ dimuon sample has a lower average value of $x_{\rm vis}$, as expected for production off sea quarks only, while the neutrino sample is consistent with approximately equal contributions from valuence and sea quarks assumed in the calculated curve. After correction for pion and kaon decay the average values of $x_{\rm vis}$ obtained from the $\bar{\nu}$ and ν samples are (0.11 ± 0.03) and (0.20 ± 0.03), respectively.

Figure 7(a) shows the distribution of $Z_+ = p_+/(p_+ + E_H)$ for the neutrino sample. Curves are shown for two assumed forms of the fragmentation function $F(Z)$ for charm particle production. Any distribution falling much faster than $\exp(-3Z)$ is rejected by the data, which show a slight preference for a flat distribution or one slowly rising with Z. Figure 7(b) shows the measured distribution of

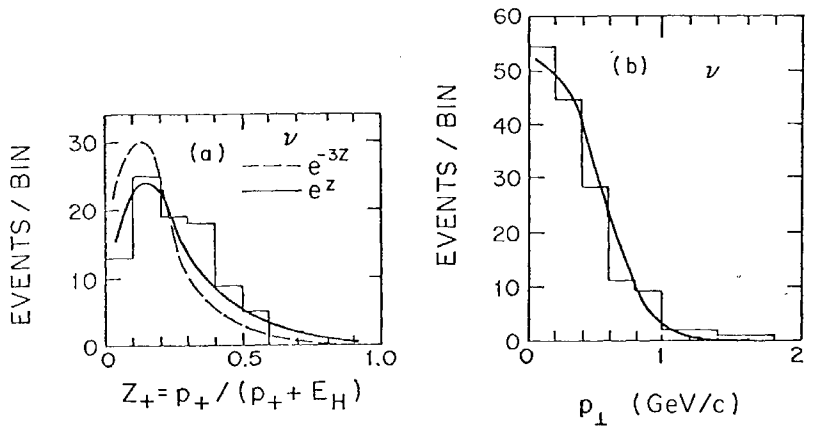

Fig. 7. Neutrino-induced dimuon distributions in (a) Z_+ and (b) $p_\perp$ compared with charm model predictions. One event is off scale in $p_\perp$ in (b).

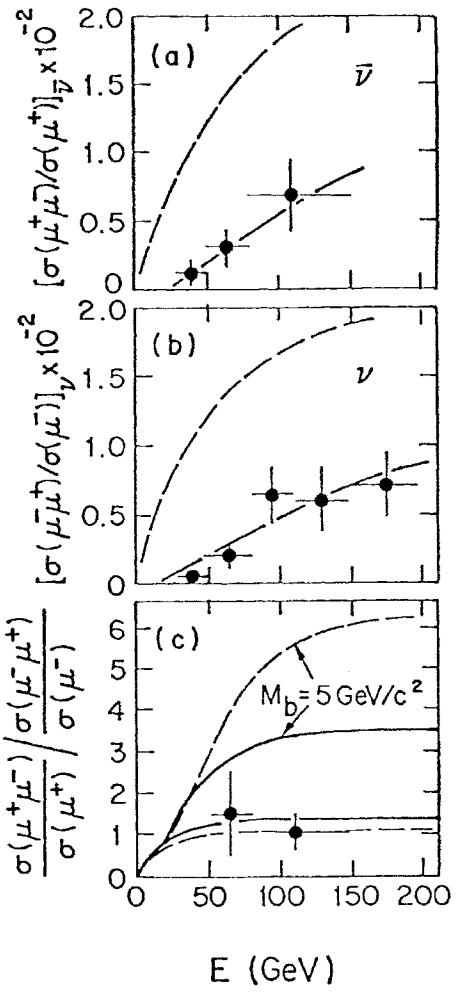

Fig. 8. Measured ratio of dimuon to single muon rates (corrected for π and K decays) as a function of energy for (a) $\bar{\nu}$ and (b) ν. The errors shown are statistical only. The curves are from a charm model calculation with a 5 GeV/c minimum muon momentum requirement (solid) and without that requirement (dashed). (c) The ratio $[\sigma(\mu^+\mu^-)/\sigma(\mu^+)]/[\sigma(\mu^-\mu^+)/\sigma(\mu^-)]$ as a function of energy. The dashed curves are for the standard four-quark model and for additional 5 GeV/c^2 b-quark production and decay. The solid curves include estimated asymptotic freedom corrections to those alternatives. The curves are from Barnett and Martin [Phys. Rev. **D16** (1977) 2765].

$p_\perp$ for the neutrino sample, where $p_\perp$ is the momentum component of the μ^+ perpendicular to the plane formed by the incoming ν and the outgoing μ^-. The curve is obtained assuming D mesons are produced with a momentum transverse to the W direction of the form $dN/dp_t^2 = \text{const}\ \exp[-6(p_t^2+m_D^2)^{1/2}]$. Both Figs. 6 and 7 show good agreement of the data with the charm model.

The measured ratios of dimuon to single muon events, corrected for pion and kaon decay, are shown as functions of energy in Figs. 8(a) and (b) for $\bar{\nu}$ and ν, respectively. The curves show the energy dependence expected from the charm calculation with and without the 5 GeV/c minimum muon momentum requirement. Above 80 GeV, the ratio of dimuon to single muon events is $(0.65\pm 0.13)\ 10^{-2}$ for ν and $(0.70\pm 0.25)\ 10^{-2}$ for $\bar{\nu}$, with the 5 GeV/c minimum momntum cut.

The magnitude of the strange quark fractional momentum can be extracted from the measured dimuon rates and data on single muon production by $\bar{\nu}$ and ν at high energy. Noting that the target of the experiment is isoscalar ($U=D$, where U, D are the fractional momenta carried by the u, d quarks), one determines the ratios $\bar{S}/U$ and S/D independently from the $\bar{\nu}$ and ν dimuon data of Figs. 8a and b after correcting for the minimum muon momentum requirement. This correction is sensitive to the Z-distribution assumed for charm production. We have taken a flat Z-distribution consistent with Fig. 7a. If we use instead the ratio $[\sigma(\mu^+\mu^-)/\sigma(\mu^+)]/[\sigma(\mu^-\mu^+)/\sigma(\mu^-)]$ from Fig. 8c, we obtain S/D, independent of any correction for dimuon acceptance. The results are given in Table II. We also include in Table II the value of $\bar{D}/D$.

Table II. Values of the fractional momentum carried by the strange quarks and by the ordinary antiquarks obtained from the *data above 80 GeV* of the HPWF (310) experiment.

Ratio	Value
S/U	0.076 ± 0.027
S/D	0.099 ± 0.035
$\bar{S}/D$	0.066 ± 0.061
$\bar{D}/D=\bar{U}/U$	$0.13\ \pm0.03$

Figure 8(c) compares the measured energy dependence of the ratio $[\sigma(\mu^+\mu^-)/\sigma(\mu^+)]/[\sigma(\mu^-\mu^+)/\sigma(\mu^-)]$ with the calculated dependence assuming charm only, and assuming a right-handed, full strength coupled, charge $-1/3$ (b-) quark in addition. The latter quark, with a mass in the vicinity of 5 GeV/c^2, seems to be ruled out by more than 4 standard deviations, but this conclusion is subject to uncertainities in the calculated large asymptotic freedom correction.

In summary, the opposite sign dimuon data presented here are consistent in all respects with the production and decay of charm particles, although a contribution from

other sources at the level of roughly 20% cannot be excluded. Within experimental error, the strange quarks seem to carry a smaller fraction of the nucleon momentum than the ordinary antiquarks. Finally, there is no evidence in these dimuon data for a charge $-1/3$ quark of mass 5 GeV/c^2 with right-handed, full strength coupling to a u-quark.

§3. $\nu_\mu(\bar{\nu}_\mu)+N\to\mu^\mp+\mu^\mp+X$

The nature and origin of observed like-sign dimuon events remain unknown. We know that much of the observed rate of like-sign dimuons is due to the decay in flight of pions and kaons from ordinary deep inelastic neutrino events. It is important, however, to determine whether "prompt" like-sign events exist. We report here on a data sample about seven times larger than our former sample which yields a relative rate $N(\mu^-\mu^-)/N(\mu^-\mu^+)$ that suggests the presence of a prompt $\mu^-\mu^-$ signal.

For the like-sign dimuon measurements, the significant aspect of the E-310 apparatus is that it consists of three target-detectors of different density, an iron target (FeT), a liquid scintillator calorimeter (LiqC) and an iron-plate calorimeter (FeC). The fiducial mass and absorption lengths of these targets are: FeT, 198 tons and 31 cm; LiqC, 36 tons and 120 cm; FeC, 42 tons and 61 cm.

The relative rates $R(\mu^-\mu^-)/R(\mu^-)$ in each target are difficult to determine because of differences in acceptance and trigger requirements between dimuons and single muon events. However, the ratio $N(\mu^-\mu^-)/N(\mu^-\mu^+)$ was verified to be independent of these systematic effects. The ratios $N^{\rm obs}(\mu^-\mu^-)/N^{\rm obs}(\mu^-\mu^+)$ plotted against hadronic absorption length are shown in Figs. 9a and b for muon momentum cuts $p_\mu>5$ and 10 GeV/c, respectively. To simplify the interpretation, the fraction of $\mu^-\mu^+$ events due to pion and kaon decays should be subtracted from $N^{\rm obs}(\mu^-\mu^+)$. This background is obtained from a calculation which uses among other data momentum spectra and multiplicities of charged pions and kaons measured in neutrino interactions. The ratios $N^{\rm obs}(\mu^-\mu^-)/N^{\rm prompt}(\mu^-\mu^+)$ obtained after this correction should then exhibit only the dependence on absorption length of the observed $\mu^-\mu^-$ events. This is shown in

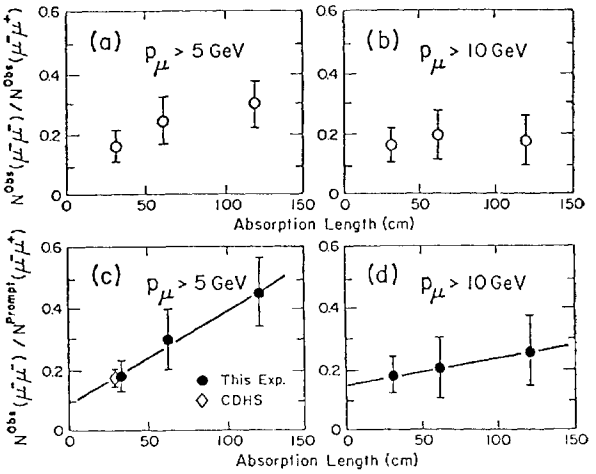

Fig. 9. Ratios of the number of observed $\mu^-\mu^-$ events to $\mu^-\mu^+$ events in three targets of different hadronic absorption lengths for (a) $p_\mu>5$ GeV and (b) $p_\mu>10$ GeV. Also shown are ratios of the number of observed $\mu^-\mu^-$ events to the number of *prompt* $\mu^-\mu^+$ events versus hadronic absorption length for (c) $p_\mu>5$ GeV and (d) $p_\mu>10$ GeV. The straight line is a linear fit to the data of this experiment.

Figs. 9c and d. Linear fits to the data, with both the slope and intercept as free parameters, are also shown.

We observe that i) the decay of pions and kaons account for a significant fraction of the $\mu^-\mu^-$ events for the case $p_\mu>5$ GeV/c; ii) the fitted slope decreases by a factor of about 4 as the minimum momentum cut of the muons is raised from 5 to 10 GeV/c. This factor of 4, which results from the reduction of pion and kaon background as the momentum cut-off is increased, is verified in our detailed calculation of pion and kaon decay. Note that the fitted slopes empirically determine the pion and kaon decay contributions to the $\mu^-\mu^-$ events. The value of the fitted slope for the $p_\mu>5$ GeV/c data in Fig. 9c is $(3.0\pm1.3)\times10^{-3}$ cm^{-1}, in agreement with the value $(4.0\pm1.0)\times10^{-3}$ cm^{-1} obtained from the calculated numbers $N^{\rm decay}(\mu^-\mu^-)$. This agreement gives us confidence in using the decay in flight calculation to determine the magnitude of the prompt $\mu^-\mu^-$ signal in each target for the $p_\mu>10$ GeV/c data. The ratios $N^{\rm prompt}(\mu^-\mu^-)/N^{\rm prompt}(\mu^-\mu^+)$ shown in Figure 10 are seen to be systematically non-zero and independent of absorption length. Averaging over all three targets we obtain $N^{\rm prompt}(\mu^-\mu^-)/N^{\rm prompt}(\mu^-\mu^+)=0.12\pm0.05$ for $p_\mu>10$ GeV/c.

What are possible origins of prompt $\mu^-\mu^-$

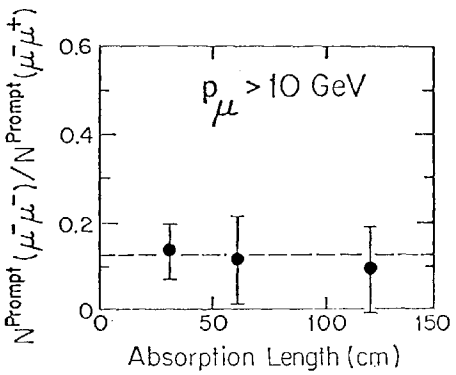

Fig. 10. Number of prompt $\mu^-\mu^-$ events relative to the number of prompt $\mu^-\mu^+$ events in each of the three targets for $p_\mu > 10$ GeV.

events? Only $\mu^-\mu^+$ are expected if charm particles are produced *singly* by neutrinos. Any mechanism to explain the $\mu^-\mu^-$ events that invokes new physics beyond charm must be measured against the following alternatives: (a) radiative or direct muon pair production in deep inelastic charged-current interactions, (b) associated production of charmed particles. However, $\mu^-\mu^-$ events could result from the mechanisms in (a) only if the μ^+ escapes experimental detection. Calculations for mechanisms (a) lead to $R(\mu^-\mu^-)/R(\mu^-\mu^-\mu^+) < 1$, contrary to the experimental observation. Therefore, mechanism (a) is not likely to be the dominant source of like-sign dimuon events. Both $\mu^-\mu^-$ and $\mu^-\mu^-\mu^+$ are expected from associated charm production. The ratio $R(\mu^-\mu^-\mu^+)/R(\mu^-\mu^-)$ is expected to be roughly $BR(C\to\mu+\nu+X)\simeq 0.1$, which is compatible with our observed ratio.

In summary, we have presented evidence for the possible production of prompt like-sign dimuons ($\mu^-\mu^-$) by neutrinos. The rate of prompt $\mu^-\mu^-$ events relative to the prompt $\mu^-\mu^+$ events is measured to be 0.06 ± 0.05 for $p_\mu > 5$ GeV/c, and 0.12 ± 0.05 for $p_\mu > 10$ GeV/c. The observed properties of the $\mu^-\mu^-$ events are similar to those of the $\mu^-\mu^+$ events and are therefore consistent with a hadronic origin. We have no evidence for prompt $\mu^+\mu^+$ events produced by antineutrinos.

§4. $\nu_\mu + N \to \mu^- + \mu^- + \mu^+ + X$

The distribution of trimuon events observed to date in E-310 is shown in Table III. There are an additional 15 events with at least one muon with momentum below 2 GeV/c. The two events ($-++$) are consistent with dimuon production plus pion or kaon decay.

Table III. Number of trimuon events for each target for $p_\mu > 2$ GeV/c. Numbers in parentheses indicate a 4.5 GeV/c cut.

	3Q		2Q		
	$--+$	$-++$	$--?$	$-+?$	$++?$
FeT	10 (9)	1 (1)	5 (2)	7 (1)	0
LiQ	10 (5)	0	7 (0)	4 (0)	0
FeC	6 (4)	1 (0)	0	0	0

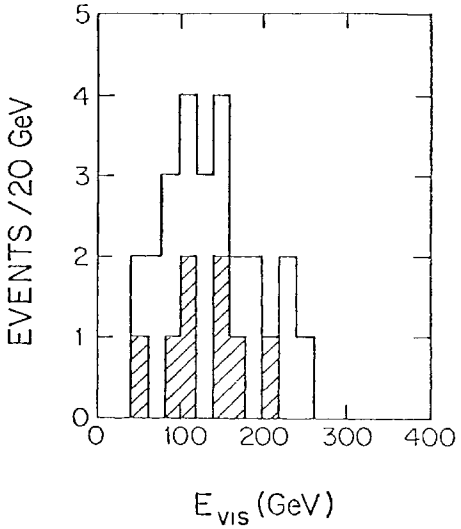

Fig. 11. Visible energy of the trimuon events.

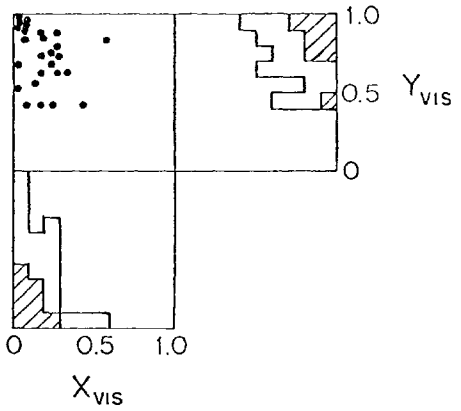

Fig. 12. Scatter plot of x_{vis} and y_{vis} of the trimuon events.

The distribution in E_{vis} for these trimuon events is shown in Fig. 11 where it is seen that 3/4 of the events have $E_{vis} > 100$ GeV, which is a result of the hard neutrino spectra used in E-310. For brevity's sake, we suppress other dynamic distributions, except for x_{vis} and y_{vis} for these events, which are shown in Fig. 12 and look as expected for neutrino-induced inelastic interactions.

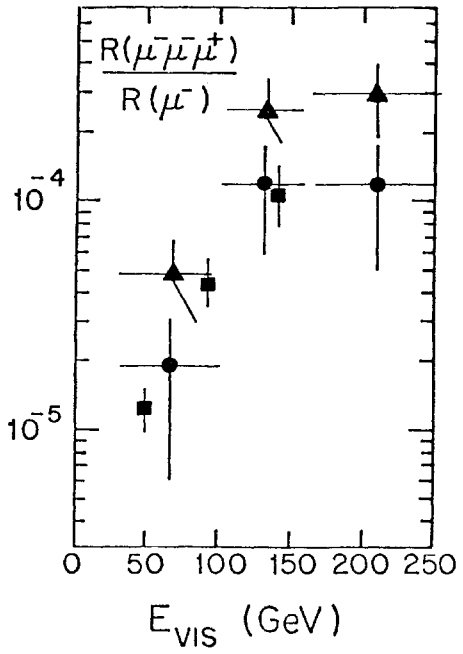

Fig. 13. Trimuon rates as a function of visible energy. The triangles and circles are from HPWF E-310 with $p_\mu > 2$ GeV/c and $p_\mu > 4.5$ GeV/c, respectively. The squares are CDHS data with $p_\mu > 4.5$ GeV/c.

The relative rates $R(\mu^-\mu^-\mu^+)/R(\mu^-)$ from E-310 for $p_\mu > 2$ GeV/c and $p_\mu > 4.5$ GeV/c are shown as functions of energy in Fig. 13. There is good agreement, seen in Fig. 13, between the results of this experiment and those of the CDHS experiment. Measured multimuon rates, *i.e.*, dimuon, trimuon, and tetramuon rates, from E-310 are given in Table IV.

We briefly summarize the conclusions relating to the trimuon events observed in E-310 as follows:

1. Most $\mu^-\mu^-\mu^+$ events arise from a current neutrino interaction with
   (a) direct production of $\mu^-\mu^+$ at the hadron vertex;
   (b) radiative production of $\mu^-\mu^+$ from the initial μ^-(q);
   (c) possibly (10–20)% charm-anticharm production.
2. New quark, new lepton production does not exceed 10^{-5} of all ν-interactions with $E_\nu \gtrsim 150$ GeV.
3. The two "exotic" trimuon events with very high total muon energy observed earlier remain valid and unexplained. We would have expected 2 or 3 more such events in E-310; only one candidate for this class was observed.

Table IV. Multimuon rates with momentum cuts given in the text.

	All E_ν	$E_\nu > 100$
$R(\mu^-\mu^+)/R(\mu^-)$	$4.0\pm0.8\times10^{-3}$	$6.5\pm1.3\times10^{-3}$
$R(\mu^+\mu^-)/R(\mu^+)$	$2.7\pm0.9\times10^{-3}$	$7.0\pm2.5\times10^{-3}$
$R(\mu^-\mu^-)/R(\mu^-)$	$4.0\pm2.0\times10^{-4}$	$6.5\pm3.5\times10^{-4}$
$R(\mu^+\mu^+)/R(\mu^+)$	$\lesssim10^{-4}$	—
$R(\mu^-\mu^-\mu^+)/R(\mu^-)$	$6\pm2\times10^{-5}$	$1.2\pm0.5\times10^{-4}$
$R(4\mu)/R(\mu^-)$	$\lesssim7\times10^{-6}$	—
$R(<4\mu)/R(\mu^-)$	$<5\times10^{-6}$	—

The results presented here were obtained by members of the E-310 collaboration from Fermilab, Harvard, Ohio State, University of Pennsylvania, Rutgers, and University of Wisconsin. The members are: A. Benvenuti*, F. Bobisut**, D. Cline, P. S. Cooper†, M. G. D. Gilchriese††, S. M. Heagy, R. Imlay, M. E. Johnson, T. Y. Ling, R. Lundy, P. McIntyre, S. Mori, D. D. Reeder, J. A. Rich, R. Stefanski, and D. R. Winn.

* Now at CERN, Geneva, Switzerland.

** Visitor at the University of Pennsylvania; permanent address Istituto di Fisica dell' Universita, Padova, Italy.

† Now at Department of Physics, Yale University.

†† Now at Department of Physics, Cornell University.